Dalton Transactions

Accepted Manuscript

ROYAL SOCIETY OF CHEMISTRY

www.rsc.org/dalton

Type-II clathrate of $Cs_8Na_{16-x}Tl_xGe_{136}$ was synthesized.

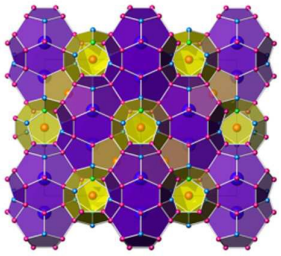

Journal Name

ARTICLE

Structure and Properties of type-II Clathrate $Cs_8Na_{16-x}Tl_xGe_{136}$

Hui Zhang[a], Wei Li[b,c], Xuguang Xu[b], Gang Mu[b], Xiaoming Xie[b] and Fuqiang Huang[a,d*]

Received 00th January 20xx,
Accepted 00th January 20xx

DOI: 10.1039/x0xx00000x

www.rsc.org/

The Tl doped type II clathrate $Cs_8Na_{16-x}Tl_xGe_{136}$ was synthesized from the elements. The structure was refined by single crystal and powder diffraction. $Cs_8Na_{16-x}Tl_xGe_{136}$ crystalized in the space group $Fd\bar{3}m$. The melting points decrease with the increasing of Tl contents at 925.0 °C, 922.8 °C and 915.7 °C for $Cs_8Na_{14.76(3)}Tl_{1.24(2)}Ge_{136}$, $Cs_8Na_{9.94(2)}Tl_{6.06(2)}Ge_{136}$ and $Cs_8Na_{8.36(2)}Tl_{7.64(2)}Ge_{136}$ in Ar atmosphere. The magnetism of $Cs_8Na_{9.94(2)}Tl_{6.06(2)}Ge_{136}$ indicates a diamagnetism with χ=-3.11×10^{-3} emu·mol^{-1} at 1.8 K. The heat capacity of $Cs_8Na_{9.94(2)}Tl_{6.06(2)}Ge_{136}$ presents an Einstein peak at 10 K. The fitted parameters for $Cs_8Na_{9.94(2)}Tl_{6.06(2)}Ge_{136}$ are λ = 0.115(4) J·mol^{-1}·K^{-2}, β = 0.0289(2) J·mol^{-1}·K^{-4}, N_E = 7.94(4), θ_E = 56.9(1) K, N_D = 152.06(4) and θ_D = 217(1) K using $C_p = C_e + C_D + C_E$ equation from 1.8 K and 10 K. The thermoelectric measurement shows metallic resistivity and negative Seebeck coefficient indicating electron-type charge carriers. The electronic structure calculation for $Cs_8Na_{10}Tl_6Ge_{136}$ confirms the nature of metallic transport behavior with conducting electrons mainly from the Ge *p* orbitals.

Introduction

The recent impetuous interests in tetrel-containing clathrate are motivated in particular by the search for a new generation of efficient thermoelectric materials. Overwhelmingly, type-I clathrates with space group $Pm\bar{3}n$ are investigated extensively. Clathrates crystallize in lots of structure types [1-5] as well as the superstructure variants [6-9]. The increased attention is also received by other type clathrates with the so called type-II clathrates ($Fd\bar{3}m$) of A_xM_{136} (A = Na, K, Rb, Cs, Ba; M=Si, Ge; *x* = 0-24) [10-21], type-III clathrates (space group $P4_2/mnm$) of $A_{30}Na_{(1.33x-10)}Sn_{(172-x)}$ (A = Cs or Cs/Rb) [22] and $Si_{130}P_{42}Te_{21}$ [23], type-VIII clathrates (space group $I\bar{4}32$) of $Ba_8Ga_{17.2}Sn_{28.8}$ [24] and $Eu_8Ga_{16}Ge_{30}$ [25], as well as type-IX clathrates (space group $P4_132$) of K_8Sn_{25} [26] and Ba_6Ge_{25} [27].

Clathrate compounds comprise host frameworks that embrace guest species in polyhedral cages. They can be classified by the charge distribution between the framework and guest as anionic, cationic and neutral clathrates. In anionic clathrates [1-22,24-27], cations of alkali- or alkaline-earth, or europium balance the negatively charged framework, while, in the cationic clathrates, the negative charges of halogen, selenium or tellurium guest anions are compensated by positive charges of the framework based on Si, Ge, or Sn accompanied by pnicogen, selenium, tellurium, or even iodine [28-31]. Ge_{136} presents a neutral clathrate [10].

In clathrate Ba_8Ge_{43} [32] and Ba_8Ge_{40} [33] there exist defects in the framework. Thallium in the framework has been found in fulfilled clathrate-I $Ba_8(Ba_{2.4}Tl_{7.2}Ge_{36.4})$ [34]. In $Ba_8(Ba_{2.4}Tl_{7.2}Ge_{36.4})$ structure Ba1 and Ba2 locate in big and small cages, Ge1, Ge2 and Tl1/Ba3/Ge3 occupy three crystallographic sites in the framework, respectively. Thallium in the cages alone or with Na are also discovered in zeolites of $Tl_{12}(Al_{12}Si_{12}O_{48})$ [35] and $Tl_8Na_4(Al_{12}Si_{12}O_{48})$ [36]. To reveal the nature of Tl location in clathrates-II, we, in the present work, report synthesis and properties of type-II clathrate $Cs_8Na_{16-x}Tl_xGe_{136}$, where Tl incorporates only in the small cages with Na.

Experimental

Synthesis. Mixtures of Cs (99.9%), Na (99.9%), Tl (99.99%) and Ge (99.9999%) with a mole ratio Cs : Na : Tl : Ge = 8 : 16-n : n : 136 (n=0, 4, 8, 12, 16) with the total mass approximating to 1 g were welded in tantalum tube in an argon-filled glovebox ($c(O_2)$ and $c(H_2O)$ ≤ 1 ppm), then sealed in a quartz ampoule in vacuum and finally heated at 600 °C for 1 week. $Cs_8Na_{16}Ge_{136}$ [15] was prepared for comparison (n=0). The unreacted dark grey Ge particles were picked out and the by-products of binary dark powders of CsGe, TlGe and NaGe were washed off using water. The left grey blocks were washed with eternal further and then dried at 80 °C for 12 h.

[a] CAS Key Laboratory of Materials for Energy Conversion and State Key Laboratory of High Performance Ceramics and SuperfineMicrostructures,Shanghai Institute of Ceramics, Chinese Academy of Sciences, Shanghai 200050, P. R. China.
[b] State Key Laboratory of Functional Materials for Informatics and Shanghai Center for Superconductivity, Shanghai Institute of Microsystem and Information Technology, Chinese Academy of Sciences, Shanghai 200050, P. R. China.
[c] State Key Laboratory of Surface Physics and Department of Physics, Fudan University, Shanghai 200433, P. R. China.
[d] Beijing National Laboratory for Molecular Sciences, College of Chemistry and Molecular Engineering, Peking University, Beijing 100871, P. R. China.
Electronic Supplementary Information (ESI) available: [CSD1062647,CSD1411481-1411483]. See DOI: 10.1039/x0xx00000x

The sample (n=8) for transport measurement was hot pressure sintered at 300 °C for 3h.

Morphology and composition analysis. The metallography of the specimens was investigated with a Philips XL 30 scanning electron microscope (LaB_6 cathode). Energy dispersive X-ray spectroscopy (EDXS) was performed with the Si (Li) detector of an EDAX system (Gemsis Software V 4.61). The element composition was calculated from the measured intensities of the X-ray lines Cs *L*, Na *K*, Tl *L* and Ge *K* caused by the electron beam at 25 kV acceleration voltage by the standard-less method using the ZAF matrix correction.

Differential scanning calorimetry. DSC measurements were performed with a Netzsch DSC 404 C instrument. About 20 mg of sample in a glassy carbon crucible (∅ 4 mm, *l* = 6 mm, Sigradur G, HTW) were sealed in Nb ampoules (∅ 5 mm). The system was heated under Ar atmosphere from room temperature to 1473 K by applying heating rates 5 K/min.

X-ray single crystal diffraction. Single crystal was mechanically separated from the polycrystalline product (n=8). The crystal was fixed on top of glass capillary with grease. Diffraction data were collected with a rotating anode diffraction system, RIGAKU RAXIS Spider (Varimax optical system, Ag Kα radiation, λ = 0.56084 Å). Absorption correction was performed with a multi-scan procedure. All crystallographic calculation was performed on SHELXL-2014 package [37]. For the structure presentation ATOMS V 6.0 was used [38].

X-ray powder diffraction. X-ray powder diffraction dada collections were performed on Huber G670 Image Plate Camera ($CuK_{\alpha1}$ radiation, λ = 1.540598 Å). The structures of powder samples were resolved by direct method using *WinCSD* package [39].

Physical properties. Magnetization was measured in external fields of 20 Oe and 7 T from 1.8 to 400 K with MPMS XL-744 (Quantum Design). The contribution of the sample holder was subtracted. The heat capacity and thermoelectric transport from 1.8 to 400 K were measured in a physical property measurement system, PPMS (Quantum Design).

First-Principles calculation. The first-principles calculation was carried out by means of the density functional theory using the pseudopotential as implemented in the VASP code [40]. The exchange-correlation potential was calculated using the generalized gradient approximation (GGA) as proposed by Perdew Burke Ernzerhof [41]. Throughout the calculations, a 500 eV cutoff in the plane wave expansion and a 4×4×4 Monkhorst-Pack **k** grid were chosen to ensure the calculation with an accuracy of 10^{-5} eV. Furthermore, those calculations were performed using the experimental crystal structure.

Results and discussion

Morphologies and compositions. The obtained $Cs_8Na_{16}Ge_{136}$, $Cs_8Na_{14.76(3)}Tl_{1.24(2)}Ge_{136}$, $Cs_8Na_{9.92(2)}Tl_{6.08(2)}Ge_{136}$ and $Cs_8Na_{9.36(2)}Tl_{7.64(2)}Ge_{136}$ (nominal n=0, 4, 8, 12) are grey blocks. $Cs_8Tl_{16}Ge_{136}$ (n=16) does not exist. From SEM images (Fig. 1) one can see that $Cs_8Na_{16}Ge_{136}$ and $Cs_8Na_{14.76(3)}Tl_{1.24(2)}Ge_{136}$ have clear facets. In $Cs_8Na_{9.92(2)}Tl_{6.08(2)}Ge_{136}$ the facets melt together. $Cs_8Na_{9.36(2)}Tl_{7.64(2)}Ge_{136}$ looks as broken blocks.

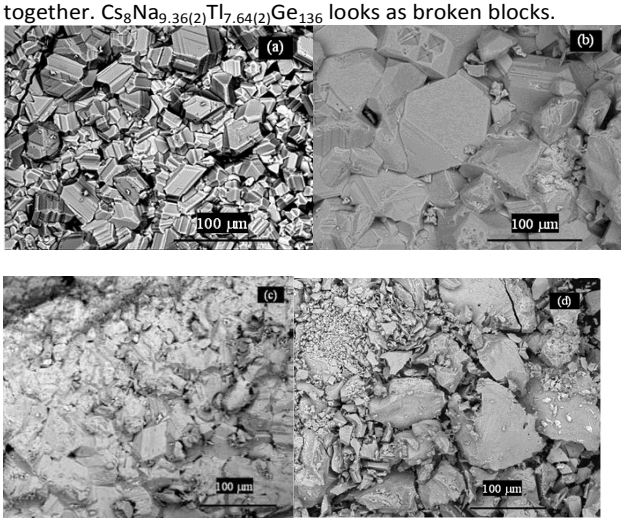

Figure 1. SEM morphorlogy of $Cs_8Na_{16}Ge_{136}$ (a), $Cs_8Na_{14.76(2)}Tl_{1.24(2)}Ge_{136}$ (b), $Cs_8Na_{9.94(2)}Tl_{6.06(2)}Ge_{136}$ (c), and $Cs_8Na_{8.36(2)}Tl_{7.64(2)}Ge_{136}$ (d).

EDX gives the compositions of $Cs_{7.9(1)}Na_{8(2)}Tl_{6.3(1)}Ge_{136.0(3)}$ for powders and $Cs_{7.9(1)}Na_{8(2)}Tl_{6.3(1)}Ge_{136(3)}$ for single crystal for the nominal composition of $Cs_8Na_8Tl_8Ge_{136}$ sample. The larger relative standard errors lie in the atom numbers of Na than that of Tl for the light mass of Na and heavy mass of Tl as well as the residual Tl. The sites of Cs and Ge are fulfilled. The final compositions of the samples are determined by structure refinement of single crystal and powders.

Melting points. The melting points of $Cs_8Na_{16}Ge_{136}$, $Cs_8Na_{14.76(3)}Tl_{1.24(2)}Ge_{136}$, $Cs_8Na_{9.94(2)}Tl_{6.06(2)}Ge_{136}$ and $Cs_8Na_{9.36(2)}Tl_{7.64(2)}Ge_{136}$ are 936.9 °C, 925.0 °C, 922.8 °C and 915.7 °C deduced from DSC analysis. Their melting points are a little lower than that of element Ge of 937.4 °C. One can see that the melting points are mainly determined by the framework atoms of Ge and with Tl content increasing the melting points decrease for a few degrees.

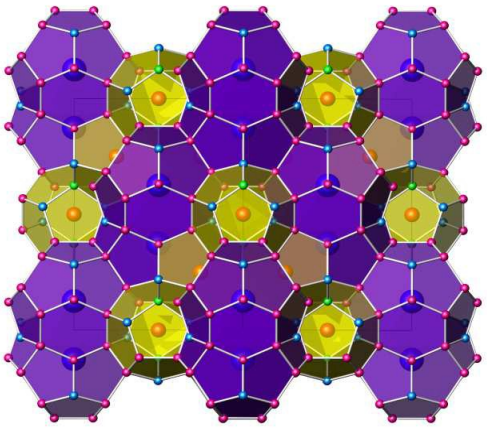

Fig. 2 Type-II clathrate structure of $Cs_8Na_{9.94(2)}Tl_{6.06\ (2)}Ge_{136}$: pink Tl/Na (8*b*) and blue Cs (16*c*) lie in the center of yellow and violet 20-vertex pentagonal dodecahedra [5^{12}] and 28-vertex

hexakaidecahedra [$5^{12}6^4$] built by Ge1 (green, at 8*a*), Ge2 (blue, at 32*e*) and Ge3 (red, at 96*g*).

Structural determination. A single crystal was picked up from the nominal *n* = 8 sample refined as $Cs_8Na_{10.24(2)}Tl_{5.76(2)}Ge_{136}$. The single crystal structure of $Cs_8Na_{10.24(2)}Tl_{5.76(2)}Ge_{136}$ was solved by direct method using SHELXL-2014[37]. The crystal crystalized in the space group $Fd\bar{3}m$ (no. 227) with lattice parameters a = 15.5227(10) Å refined with θ range from 3.59° to 34.10°. The direct method allowed the localization of all atomic positions in a type-II clathrate structure. At first the three distinct crystallographic sites of the 96g, 32e and 8a in the framework were set as Ge, using the Wyckoff notation. The two distinct guest atom sites, the 8b site of the large cage, and 16c site of the small cage were considered to be occupied by Cs and Na, respectively. The refinement indicated negative atomic displacement parameters (ADPs) for Na in 16c. The 16c site was considered to have mixed occupancy of Na and Tl. All atoms in the crystal structure were refined using anisotropic ADPs. The final anisotropic refinement of all atoms leaded to the composition $Cs_8Na_{10.24(2)}Tl_{5.76(2)}Ge_{136}$ with *R* = 2.64%. The details crystal data, data collection and structure refinement, and atomic parameters are presented in Tables 1-2, respectively. Fractional atomic coordinates and isotropic or equivalent isotropic displacement parameters (Å^2), and anisotropic displacement parameters U_{ij} (Å^2) for $Cs_8Na_{10.24(2)}Tl_{5.76(2)}Ge_{136}$ are listed in Table 3 and 4. Selected interatomic distances and angles (Å, °) for $Cs_8Na_{10.24(2)}Tl_{5.76(2)}Ge_{136}$ single crystal are given in Table 5.

We have considered the possibility of Tl within the framework of Ge or in Cs position. But the refinement the occupancy of Ge or Cs does not deviate from 1. Tl and Na atom both transfers electrons to the framework. The difference lies in that this electron is from Tl $6s^26p^1$ or Na $3s^1$. That goes along with the known conventions in clathrate chemistry. Tl and Ba form the framework atom to elude the defects of framework in Ba_8Ge_{43}[32] or $BaGe_5$[33] and build fulfilled clathrate-I clathrate-I $Ba_4(Ba_{1.2}Tl_{3.6}Ge_{18.2})$ [34]. In $Tl_{12}(Al_{12}Si_{12}O_{48})$ and $Tl_8Na_4(Al_{12}Si_{12}O_{48})$ zeolites thallium locates in the cages of $[Al_{12}Si_{12}O_{48}]$ [35-36] alone or with Na like in Tl in small cages of $Cs_8Na_{10.24(2)}Tl_{5.76(2)}Ge_{136}$ with Na.

Structural description. The atomic arrangement of $Cs_8Na_{10.24(2)}Tl_{5.76(2)}Ge_{136}$ is a typical clathrate-II structure as $Cs_8Na_{16}Ge_{136}$ [15]. 136 four-coordinate Ge atoms build the host framework with the cages filled by Cs atoms in big cages of hexakaidecahedra [$5^{12}6^4$], Na/Tl atoms in small cages of pentagonal dodecahedra [5^{12}]. Both cages have twelve pentagonal faces, but they differ in the number of hexagonal faces, and therefore in size: a 20- vertex cage [5^{12}] filled by Na and Tl and a 28-vertex cage [$5^{12}6^4$] filled by Cs. The cages occur in the ratio 8:16 resulting in 24 cavities per unit cell available for the guest atoms for formation of the dense packed arrangement $Cs_8Na_{10.24(2)}Tl_{5.76(2)}Ge_{136}$ (Fig. 2). These polyhedra [$5^{12}6^4$] and [5^{12}] act as structural building block, sharing faces to form the type II clathrate crystal structure.

Powder refinement. The lattice parameters and structure of $Cs_8Na_{16}Ge_{136}$, $Cs_8Na_{14.76(3)}Tl_{1.24(2)}Ge_{136}$, $Cs_8Na_{9.94(2)}Tl_{6.06(2)}Ge_{136}$ and $Cs_8Na_{9.36(2)}Tl_{7.64(2)}Ge_{136}$ (from n = 0, 4, 8, 12) are refined using WinCSD package on the powder XRD patterns (Fig. 3). Even with 12 Tl in the starting composition the refined Tl content is less than 8 in $Cs_8Na_{9.36(2)}Tl_{7.64(2)}Ge_{136}$. The refined unit cell parameters, compositions, *R* factors and atom parameters for $Cs_8Na_{16}Ge_{136}$, $Cs_8Na_{14.76(2)}Tl_{1.24(2)}Ge_{136}$, $Cs_8Na_{9.94(2)}Tl_{6.06(2)}Ge_{136}$ and $Cs_8Na_{9.36(2)}Tl_{7.64(2)}Ge_{136}$ are given in Table 5. Selected interatomic distances and angles (Å, °) for $Cs_8Na_{16}Ge_{136}$, $Cs_8Na_{14.76(2)}Tl_{1.24(2)}Ge_{136}$, $Cs_8Na_{9.94(2)}Tl_{6.06(2)}Ge_{136}$ and $Cs_8Na_{8.36(2)}Tl_{7.64(2)}Ge_{136}$ powders are given in Table 4 appending to the data of single crystal $Cs_8Na_{10.24(2)}Tl_{5.76(2)}Ge_{136}$. The lattice parameters are a=15.48929(4) Å, a=15.48318(5) Å, a=15.49373(5) Å and a=15.48630(5) Å for $Cs_8Na_{16}Ge_{136}$, $Cs_8Na_{14.76(2)}Tl_{1.24(2)}Ge_{136}$, $Cs_8Na_{9.94(2)}Tl_{6.06(2)}Ge_{136}$ and $Cs_8Na_{9.36(2)}Tl_{7.64(2)}Ge_{136}$ powders. The lattice parameter has a small variation for single crystal (a=15.5227(10) Å) and powder (a=15.49373(5) Å) from n = 8. Because the refined θ angle ranges are from 3.59 to 34.10 ° for single crystal and from 4.00 to 50.00 ° for powder. The powder sample has higher θ angle range with the lower lattice parameter than single crystal.

Table 1. Crystal data for $Cs_8Na_{10.24(2)}Tl_{5.76(2)}Ge_{136}$

Chemical formula	$Cs_8Ge_{136}Na_{10.24}Tl_{5.76}$
Formula weight	12350.88 g/mol
Wavelength	0.56084 Å
Crystal size	0.020 × 0.020 × 0.020 mm
Crystal system	cubic
Space group	F d -3 m
Unit cell dimensions	a = 15.5227(10) Å
Volume	3740.3(7) Å^3
Z	1
Density (calculated)	5.483 g/cm^3
Absorption coefficient	36.952 mm^{-1}
F(000)	5371.2

Table 2. Data collection and structure refinement for $Cs_8Na_{10.24(2)}Tl_{5.76(2)}Ge_{136}$.

θ range for data collection	3.59 to 34.10°
Index ranges	-18<=h<=29, -24<=k<=22,23<=l<=31
Reflections collected	11308
Independent reflections	783 [R(int) = 0.0502]
Refinement method	Full-matrix least-squares on F^2
Refinement program	SHELXL-2014 (Sheldrick, 2014)
Function minimized	$\Sigma\, w(F_o^2 - F_c^2)^2$
Data/restraints/parameters	783 / 0 / 15
Goodness-of-fit on F^2	1.102
Δ/σ_{max}	0.000
Final R indices	707 data; I>2σ(I); R_1=0.0237, wR_2=0.0539 all data; R1=0.0264, wR2=0.0547
Weighting scheme	$w=1/[\sigma^2(F_o^2)+(0.0208P)^2+24.4551P]$ where $P=(F_o^2+2F_c^2)/3$
Absolute structure parameter	0.0(0)
Largest diff. peak and hole	1.686 and -0.934 eÅ^{-3}
R.M.S. deviation from mean	0.195 eÅ^{-3}

Journal Name

ARTICLE

Table 3. Fractional atomic coordinates and isotropic or equivalent isotropic displacement parameters (Å^2) for single crystal $Cs_8Na_{10.24(2)}Tl_{5.76(2)}Ge_{136}$.

Atom	Site	x	y	z	U_{iso}^*/U_{eq}	Occ.
Cs1	8b	1/8	1/8	5/8	0.03503(16)	1
Tl1/Na1	16c	0	0	0	0.01521(12)	0.3601(15)/0.6399
Ge1	8a	1/8	1/8	1/8	0.00948(12)	1
Ge2	32e	0.21742(2)	x	x	0.00987(7)	1
Ge3	96g	0.18226(1)	x	0.37021(2)	0.01004(6)	1

*U(eq) is defined as one third of the trace of the orthogonalized U_{ij} tensor.

Table 4. Anisotropic displacement parameters U_{ij}^* (Å^2) for single crystal $Cs_8Na_{10.24(2)}Tl_{5.76(2)}Ge_{136}$

	U_{11}	U_{22}	U_{33}	U_{12}	U_{13}	U_{23}
Cs1	0.03503(16)	0.03503(16)	0.03503(16)	0	0	0
Tl1	0.01521(12)	0.01521(12)	0.01521(12)	−0.00099(8)	−0.00099(8)	−0.00099(8)
Na1	0.01521(12)	0.01521(12)	0.01521(12)	−0.00099(8)	−0.00099(8)	−0.00099(8)
Ge1	0.00948(12)	0.00948(12)	0.00948(12)	0	0	0
Ge2	0.00987(7)	0.00987(7)	0.00987(7)	0.00001(6)	0.00001(6)	0.00001(6)
Ge3	0.00988(7)	0.00988(7)	0.01037(9)	0.00038(6)	0.00019(4)	0.00019(4)

The anisotropic atomic displacement factor exponent takes the form: $U_{ij} = -2\pi^2[\,h^2a^2U_{11} + \ldots + 2hkabU_{12}]$

Table 5. Selected interatomic distances and angles (Å, °) for $Cs_8Na_{10.24(2)}Tl_{5.76(2)}Ge_{136}$ single crystal (a) as well as $Cs_8Na_{16}Ge_{136}$(b), $Cs_8Na_{14.76(2)}Tl_{1.24(2)}Ge_{136}$(c), $Cs_8Na_{9.94(2)}Tl_{6.06(2)}Ge_{136}$(d) and $Cs_8Na_{8.36(2)}Tl_{7.64(2)}Ge_{136}$(e) powders.

	a	b	c	d	e
Cs1—12Ge3	4.1499(3)	4.1348(7)	4.1335 (6)	4.1411(7)	4.1361(9)
Cs1—12Ge3	4.2318(6)	4.2214(4)	4.2324 (4)	4.2223(4)	4.2220(6)
Cs1—2Ge2	4.2369(6)	4.2172(7)	4.2267 (7)	4.2299(7)	4.2221(9)
Na1—2Ge1	3.3608(2)	3.3535(1)	3.3522 (1)	3.3545(1)	3.3529(1)
Na1—6Ge2	3.4498(3)	3.4466(7)	3.4408 (7)	3.4430(7)	3.4437(9)
Na1—12Ge3	3.5484(3)	3.5449(5)	3.5367 (5)	3.5433(5)	3.5424(7)
Ge1—Ge2	2.4847(4)	2.4899(7)	2.4777 (7)	2.4791(7)	2.4837(9)
Ge2—Ge3	2.4942(3)	2.492(1)	2.4940 (9)	2.491(1)	2.491(1)
Ge3—Ge3	2.5137(5)	2.4942(7)	2.4847 (6)	2.4987(7)	2.4965(9)
Ge3—Ge3	2.5057(3)	2.5108(6)	2.5048 (6)	2.5123(6)	2.5077(8)
Ge2—Ge1—Ge2	109.471(1)	109.47(3)	109.47 (3)	109.47(3)	109.47(3)
Ge1—Ge2—Ge3	107.237(10)	107.08(3)	107.02 (3)	107.31(3)	107.16(4)
Ge3—Ge2—Ge3	111.611(9)	111.75(3)	111.81 (3)	111.55(4)	111.68(4)
Ge2—Ge3—Ge3	105.422(11)	105.23(3)	104.92 (3)	105.46(3)	105.29(4)
Ge2—Ge3—Ge3	108.029(10)	108.18(3)	108.24 (3)	107.96(3)	108.10(4)
Ge3—Ge3—Ge3	108.767(8)	108.89(3)	109.18 (3)	108.76(3)	108.87(4)
Ge3—Ge3—Ge3	119.835(1)	119.81(3)	119.76 (3)	119.84(3)	119.82(4)

The lattice parameters, bond lengths and angles vary in a small range prove that Tl in the cages of $Cs_8Na_{16}Ge_{136}$, $Cs_8Na_{14.76(2)}Tl_{1.24(2)}Ge_{136}$, $Cs_8Na_{9.94(2)}Tl_{6.06(2)}Ge_{136}$ and $Cs_8Na_{9.36(2)}Tl_{7.64(2)}Ge_{136}$. The lattice parameters, bond lengths and angles are determined by the framework atoms of Ge. If Tl in framework the bond lengths and angles as well as lattice parameters will change greatly for the large difference between the atom radii of Tl (1.55 Å) and Ge (1.22 Å).

Magnetic property. The magnetic susceptibility, χ(T), of $Cs_8Na_{9.98(2)}Tl_{6.06(2)}Ge_{136}$ reveals the diamagnetic behavior with $\chi_0 = -3.11 \times 10^{-3}$ emu mole^{-1} at 1.8 K and $\chi_0 = -2.84 \times 10^{-3}$ emu mole^{-1} at 400 K under 7 T (Fig. 4). No evidence for the contributions from paramagnetic or ferromagnetic impurities

is detected from this measurement. A superconductivity transition is detected at 2.4 K at 20 Oe for both field cool and Zero field cool models (inset of Fig. 4), which can be attributed to the presence of trace (0.06 % Volume) residual Tl.

Heat capacity. The measured heat capacity C_p(T) for $Cs_8Na_{9.98(2)}Tl_{6.06(2)}Ge_{136}$ is given in Fig. 5. Plotting the data as C_p/T^3 vs T reveals clear evidence of low energy Einstein mode contribution to the specific heat, which appears as a round peak at 10 K in this representation like in references [42-46]. Considering the contributions to C_p, a model comprised of a linear combination of terms is used to fit the data:

$C_p(T) \sim C_v(T) = C_e(T) + C_E(T) + C_D(T)$ (1)

Here $C_e(T) = \gamma T$ is the electronic specific heat, γ is the Sommerfeld coefficient, and

$$\gamma = \frac{1}{3}\pi^2 \kappa^2 N(E_F) \quad (2)$$

Table 5. Atomic coordinates and equivalent isotropic displacement parameters (U_{eq}) (Å^2) for $Cs_8Na_{16}Ge_{136}$, $Cs_8Na_{14.76(2)}Tl_{1.24(2)}Ge_{136}$, $Cs_8Na_{9.94(2)}Tl_{6.06(2)}Ge_{136}$ and $Cs_8Na_{8.36(2)}Tl_{7.64(2)}Ge_{136}$ powders.

Atom	Site	x	y	z	U_{eq} *	Occ.
$Cs_8Na_{16}Ge_{136}$	a=15.48929(4) Å	R_I=3.83	R_p=4.34			
Cs1	8 b	1/8	1/8	5/8	0.02922(4)	1
Na1	16 c	0	0	0	0.02536(4)	1
Ge1	8 a	1/8	1/8	1/8	0.00468(4)	1
Ge2	32 e	0.21780(4)	x	x	0.00577(4)	1
Ge3	96 g	0.18231(3)	x	0.37065(4)	0.00777(4)	1
$Cs_8Na_{14.76(2)}Tl_{1.24(2)}Ge_{136}$	a=15.48318(5) Å	R_I=6.15%	R_p=9.54%			
Cs1	8 b	1/8	1/8	5/8	0.03528(4)	1
Tl1/Na1	16 c	0	0	0	0.01815(4)	0.0768(9)/0.9232
Ge1	8 a	1/8	1/8	1/8	0.01087(4)	1
Ge2	32 e	0.21739(4)	x	x	0.01427(4)	1
Ge3	96 g	0.18173(3)	x	0.37037(4)	0.01365(4)	1
$Cs_8Na_{9.94(2)}Tl_{6.06(2)}Ge_{136}$	a=15.49373(5) Å	R_I=6.90%	R_p=8.78%			
Cs1	8 b	1/8	1/8	5/8	0.03428(6)	1
Tl1/Na1	16 c	0	0	0	0.01549(6)	0.379(1)/0.621
Ge1	8 a	1/8	1/8	1/8	0.00823(6)	1
Ge2	32 e	0.21738(5)	x	x	0.00890(6)	1
Ge3	96 g	0.18232(3)	x	0.37031(5)	0.00958(6)	1
$Cs_8Na_{8.36(2)}Tl_{7.64(2)}Ge_{136}$	a=15.48630(5) Å	R_I=6.84%	R_p=10.66%			
Cs1	8 b	1/8	1/8	5/8	0.03638(4)	1
Tl1/Na1	16 c	0	0	0	0.01702(4)	0.478(1)/0.522
Ge1	8 a	1/8	1/8	1/8	0.01086(4)	1
Ge2	32 e	0.21786(5)	x	x	0.00783(4)	1
Ge3	96 g	0.18238(3)	x	0.37039(5)	0.01135(3)	1

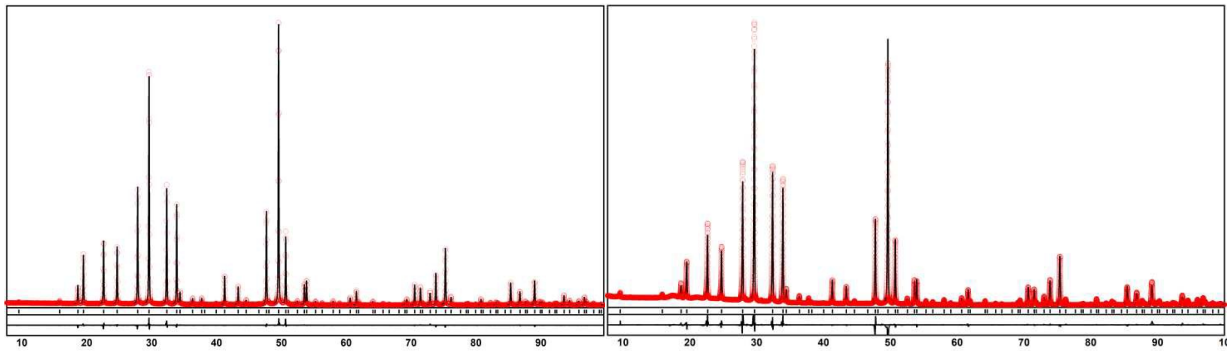

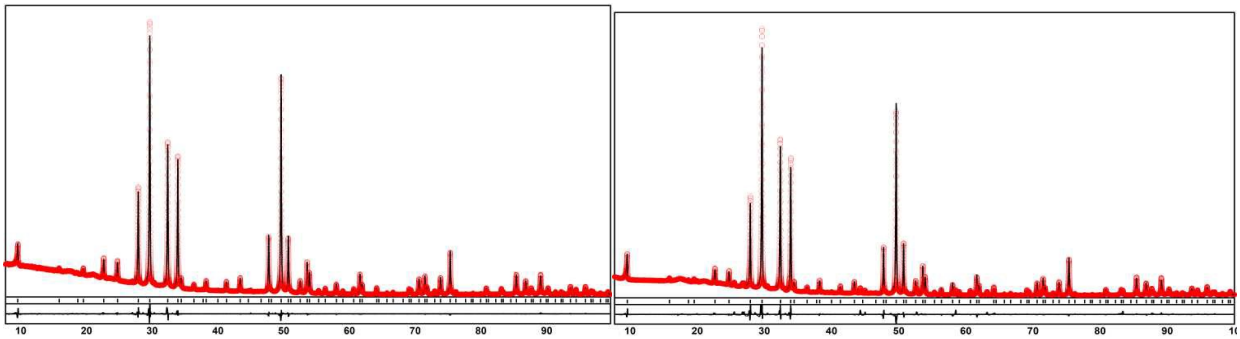

Fig. 3 Refined XRD patterns of $Cs_8Na_{16}Ge_{136}$(top left), $Cs_8Na_{14.76(2)}Tl_{1.24(2)}Ge_{136}$(top right), $Cs_8Na_{9.94(2)}Tl_{6.06(2)}Ge_{136}$(bottom left), and $Cs_8Na_{8.36(2)}Tl_{7.64(2)}Ge_{136}$ (bottom right).

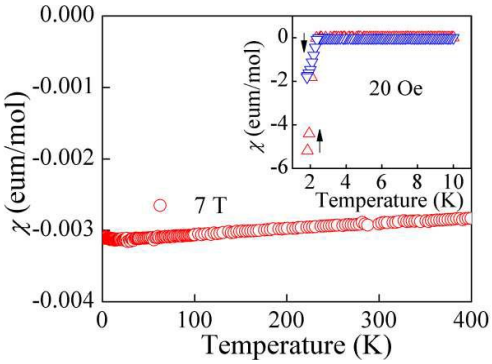

Fig. 4 Temperature dependence of the magnetic susceptibility for $Cs_8Na_{9.94(2)}Tl_{6.06(2)}Ge_{136}$ under the field 7 T, inset of it shows superconductor transition temperature of 2.4 K for residual Tl.

$$C_E(T) = 3N_E R \left(\frac{\theta_E}{T}\right)^2 \frac{\exp(\theta_E/T)}{(\exp(\theta_E/T) - 1)^2} \quad (3)$$

$C_E(T)$ is Einstein oscillator contributions, where R is the gas constant, N_E and θ_E are the number (per formula unit) and Einstein temperature of oscillator. The term $C_D(T)$ is the harmonic lattice contribution.

$$C_D(T) = 9N_D R \left(\frac{T}{\theta_D}\right)^3 \int_0^{\theta_D/T} \frac{x^4 e^x}{(e^x - 1)^2} dx \quad (4)$$

$x = h\omega/k_BT$, Debye approximation $C_D(T)$ at very low temperature is as:

$$C_D(T) \cong \frac{12\pi^4}{5} N_D R \left(\frac{T}{\theta_D}\right)^3 = \beta T^3 \quad (5)$$

N_D is the number of ''Debye atoms'' per formula unit and θ_D is the Debye temperature,

$$\beta = \frac{12\pi^4 N_D R}{5\theta_D^3} \quad (6)$$

where N_D is the number of atoms per formula unit and R the gas constant. The fit parameters of λ = 0.115(4) J·mol^{-1}·K^{-2}, β = 0.0289(2) J·mol^{-1}·K^{-4}, N_E = 7.94(4), θ_E = 56.9(1) K, N_D = 152.06(4), and θ_D = 217(1) K are deduced according to $C_p = C_e + C_E + C_D$ equation from 1.8 K to 10 K. It consists to the presumption that 8 Cs atoms are Einstein oscillator, network 136 Ge and 16 Tl/Na guest atoms are Debye atoms. γ = 0.115(4) J·mol^{-1}·K^{-2} reflects a considerable electronic contribution to the specific heat, and a substantial electronic density of states at the Fermi level as well as a typical metallic compound. This corroborates the metallic transport property that will be discussed later. A linear fit to C_p/T *vs* T^2 between 3.2 K^2 and 9.6 K^2 according to $C = \lambda T + \beta T^3$ equation gives λ = 0.142(1) J·mol^{-1}·K^{-2}, β = 0.0279(2) J·mol^{-1}·K^{-4} and θ_D = 225(1) K assuming N_D = 160 without Einstein contribution.

Thermoelectric properties. As shown in Fig. 6(a), the temperature dependent electrical resistivity ρ(T) for $Cs_8Na_{9.94(2)}Tl_{6.06(2)}Ge_{136}$ reveals metallic conduction with ρ reaching the value 1.47 mΩ·cm at 360 K. An electrical

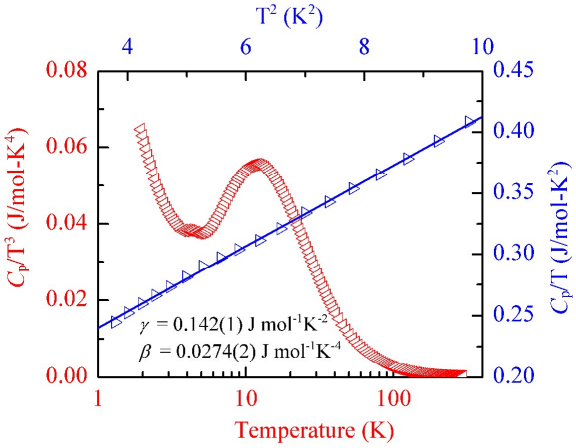

Fig. 5 Heat capacity of $Cs_8Na_{9.94(2)}Tl_{6.06(2)}Ge_{136}$ plotting as C_p/T^3 against T in the temperature range of 2 to 300 K plotted in logarithmic scale (red mark) and C_p/T against T^2 along with fitted line according to $C_p/T = \gamma + \beta T^2$ in the temperature range 3.6-10 K^2 (blue mark).

resistivity drop is detected at 2.4 K for residual Tl in $Cs_8Na_{9.94(2)}Tl_{6.06(2)}Ge_{136}$. $Cs_8Na_{9.94(2)}Tl_{6.06(2)}Ge_{136}$ reveals metallic resistivity with ρ reaching the value 1.47 mΩ·cm at 360 K. The near zero Seebeck coefficient α at 1.8 K (Fig. 6b) of $Cs_8Na_{9.94(2)}Tl_{6.06\ (2)}Ge_{136}$ decreases to the value -13 μV·K^{-1} at

360 K. The thermal conductivity κ of $Cs_8Na_{9.94(2)}Tl_{6.06\,(2)}Ge_{136}$ is shown in Fig. 6c. The total thermal conductivity increases with temperature without a peak at low temperature. The peak at low temperature is often observed in clathrate-I and which leads to a low and glass thermal conductivity. To separate the lattice κ_L and electronic κ_e contributions from the total the applied, where L is the Lorenz number ($L = 2.44\cdot10^{-8}\ V^2\cdot K^{-2}$ for

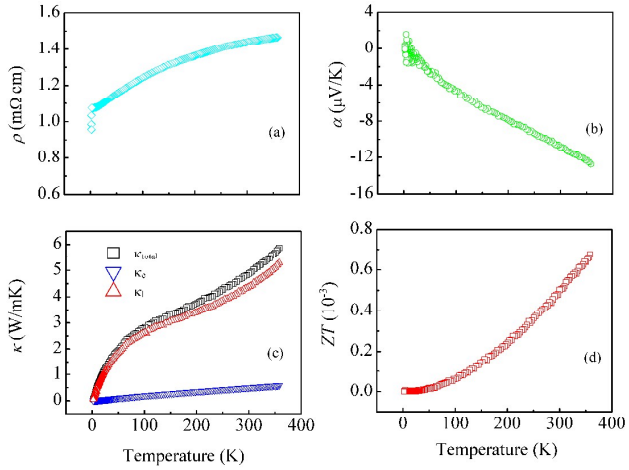

Fig. 6 Temperature dependence of the electrical resistivity ρ (a), Seebeck coefficient α (b), thermal conductivity κ (c) and thermoelectric figure of merit ZT (d) for $Cs_8Na_{9.94(2)}Tl_{6.06(2)}Ge_{136}$.

a free electron gas), T is absolute temperature and ρ *is* electric rmal conductivityκ_{total}, the Wiedemann-Franz rule $\kappa_e=LT/\rho$ is resistivity. The electronic contribution to thermal conductivity κ_e is low. The total thermal conductivity κ_{total} is mainly determined by lattice thermal conductivity κ_L. The obtained thermoelectric figure of merit ZT ($ZT=\alpha^2T/\rho\kappa$) is shown in Fig. 6d. The ZT value is low for its low Seebeck coefficient for its metallic feature.

Theoretical calculations. At last, we turn to discuss the nature of the electronic structure based on an ordered model of $Cs_8Na_{10}Tl_6Ge_{136}$ by means of the first-principle calculations. The ordered model is obtained by supposing that 6Tl exist in the inner space of the unit cell and 1 Tl at 8 corners and 9 Tl on 6 facets of the unit cell. To find the new symmetry the C2/m space group is obtained. At the same time the deduced lattice parameters of a = b = 21.9114 Å, c = 26.8359 Å and β = 144.7356 ° are obtained. The ordered structure model is given in the electronic supplementary information. The calculated total density of state (DOS) and the projected DOS on local atomic orbital are all shown in Fig. 7. It demonstrates that the system has a metallic behavior with conducting electrons mainly coming from the Ge 4*p* orbitals partially mixed with the Tl 6*p* orbitals at around the Fermi energy window ranging from -1 eV to 2 eV, which is a quite good agreement with our transport measurement shown in Fig. 5 and Fig. 6(a).

Since the typical clathrate-II $Cs_8Na_{16}Ge_{136}$ is metallic originated from the introduction the extra electrons from guest atoms [22], and the Tl could be considered as an "alkali-like" guest like Na, where Tl 6p electron and Na 3s electron mix the framework without introducing any extra electrons, the system of $Cs_8Na_{16-x}Tl_xGe_{136}$ remains the metallic phase. This point is quite good in agreement with the first-principle calculations. Generally speaking, Zintl rule is used to explain the formation of anionic

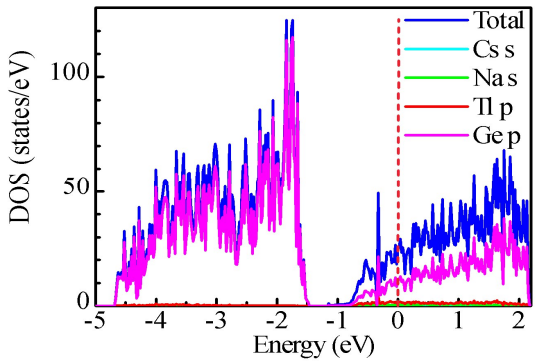

Fig. 7 The electronic structure of $Cs_8Na_{10}Tl_6Ge_{136}$ including the total DOS and projected DOS on Cs s, Na *s*, Tl *p*, and Ge *p* orbitals, evidencing a metallic behaviour with the conducting electron mainly contributed from the Ge *p* orbitals and partially from the Tl *p* orbitals.

or cationic clathrate I, where Si/Ge is partially substituted by transition metal and 13 or 15-16 group metal in the framework with introducing extra carriers [45-47]. In anionic clathrate, alkali metal or alkaline earth metal transfer electrons to transition metal, 13 group metal to form charge-balanced phase. In cationic clathrate, framework atoms 15 or 16 group elements transfer electrons to 16 or 17 group elements to fill 8 electron rules. In $Cs_8Na_{16-x}Tl_xGe_{136}$ the 136 neutral Ge have 4 bond and 4 electron configurations. The additional electrons from Cs and Na/Tl atoms lead to metallic feature. If $Cs_8Na_{16}Zn_{12}Ge_{124}$ was synthesized the guest atoms transfer 24 electrons to 12 Zn. A charge balanced Zintl phase $Cs_8Na_{16}Zn_{12}Ge_{124}$ maybe realize.

Conclusions

The thallium doped clathrates of $Cs_8Na_{14.76(3)}Tl_{1.24(2)}Ge_{136}$, $Cs_8Na_{9.94(2)}Tl_{6.06(2)}Ge_{136}$ and $Cs_8Na_{9.36(2)}Tl_{7.64(2)}Ge_{136}$ powders and $Cs_8Na_{10.24(2)}Tl_{5.76(2)}Ge_{136}$ single crystal were synthesized. They feature the complex crystal structures comprising polyhedral cages trapping Cs and Na/Tl cations. Structure refinement revealed the random distributions of thallium and sodium atoms in the small cage positions. The Tl upper limit is less than 8. The obtained clathrates show

the melt points from 915.7 to 925.0 °C, which are a little lower than 937.4°C of the melting point of element Ge. $Cs_8Na_{9.94(2)}Tl_{6.06\,(2)}Ge_{136}$ is a diamagnetic and metallic material. Heat capacity shows a clear Einstein mode and a strong electric contribution in $Cs_8Na_{9.94(2)}Tl_{6.06\,(2)}Ge_{136}$. Tl guest atoms show a high potential in clathrate chemistry and may serve as a basis for the creation of new clathrates.

Acknowledgements

This work was financially supported by the Strategic Priority Research Program (B) of the Chinese Academy of Sciences (Grants XDB04040200 and XDB04040300), the Natural Science Foundation of China (Grants 91122034, 51125006, 51202279, 61376056, 11204338, 11227902, and 11404359), Science and Technology Commission of Shanghai (Grant 13JC1405700), and Youth Innovation Promotion Association of the Chinese Academy of Sciences (No. 2015187).

Notes and references

1 T. F. Fässler, *Angew. Chem*. 2007, **119**, 2624.
2 G. S. Nolas, T. J. R. Weakley, J. L. Cohn, R. Sharma, *Phys. Rev. B*, 2005, 61, 3845.
3 M. Beekman, G. S. Nolas, *J. Mater. Chem.,* 2008, **18**, 842.
4 K. A. Kovnir, A. V. Shevelkov, *Russian Chem. Rev.* 2004, **9**, 923.
5 P. Rogl, 2005, 24th International Conference on Thermoelectrics (ICT) (IEEE), 440, Clemson, SC, USA.
6 A. V. Shevelkov, K. Kovnir*, Struct. Bond*. 2011, **139**, 97–142.
7 D. Huo, T. Sakata, T. Sasakawa, M. A. Avila, M. Tsubota, F. Iga, H. Fukuoka, S. Yamanaka, S. Aoyagi, and T. Takabatake, *Phys. Rev. B*, 2005, **71**, 075113.
8 H. G. von Schnering, R. Kroener, W. Carrillo-Cabrera, K. Peters, R. Nesper, *Zeitschrift fuer Kristallographie – NCS*. 1998, **213**, 665.
9 J. Dünner, A. Mewis, Z. Anorg. Allg. Chem., 1995, 621, 191.
10 A. M. Guloy, R. Ramlau, Z. Tang, W. Schnelle, M. Baitinger, Yu. Grin, *Nature*, 2006, **443**, 320.
11 J. S. Kasper, P. Hagenmuller, M. Pouchard, C. Cros, *Science,* 1965, **150**, 1713.
12 C. Cros, M. Pouchard, P. Hagenmuller, *J. Solid State Chem.* 1970, **2**, 570.
13 H. Horie, T. Kikudome, K. Teramura, S. Yamanaka, *J. Solid State Chem.* 2009, **182**, 129.
14 A. M. Guloy, Z. Tang, R. Ramlau, B. Böhme, M. Baitinger, and Yu. Grin, *Eur. J. Inorg. Chem.* 2009, 2455.
15 S. Bobev, S. C. Sevov, *J. Am. Chem. Soc.* 1999, **121**, 3795.
16 S. Bobev, S. C. Sevov, *J. Solid State Chem.* 2000, **153**, 92.
17 J. Gryko, R. F. Marzke, G. A. Lamberton Jr, T. M. Tritt, M. Beekman, G. S. Nolas, *Phys. Rev. B* 2005, **71**, 115208/1.
18 J. Gryko, P. F. McMillan, R. F. Marzke, G. K. Ramachandran, D. Patton, S. K. Deb, O. F. Sankey, *Phys. Rev.* B, 2000, **62**, R7707.
19 T. Rachi, K. Tanigaki, R. Kumashiro, J. Winter, H. Kuzmany, *Chem. Phys. Lett.* 2005, **409**, 48.
20 M. Beekman, J. A. Kaduk, J. Gryko, W. Wong-Ng, A. Shapiro, G. S. Nolas, *J. Alloy. Comp.* 2009, **470**, 365.
21 M. Beekman, W. Wong-Ng, J. A. Kaduk, A. Shapiro, G. S. Nolas, *J. Solid State Chem.* 2007, **180**, 1076.
22 S. Bobev and S. C. Sevov, *J. Am. Chem. Soc.* 2001, **123**, 3389.
23 J. V. Zaikina, K. A. Kovnir, F. Haarmann, W. Schnelle, U. Burkhardt, H. Borrmann, U. Schwarz, Yu. Grin, A. V. Shevelkov, *Chem. Eur. J.* 2008, **14**, 5414.
24 W. Carrillo-Cabrera, R. Cardoso Gil, V.-H. Tran, Yu. Grin, Z. Kristallogr. NCS 2002, **217**, 181.
25 S. Paschen, W. Carrillo-Cabrera, A. Bentien, V. H. Tran, M. Baenitz, Yu. Grin, F. Steglich, Phys. Rev. B. 2010, **64**, 214404.
26 J. T. Zhao, J. D. Corbett, *Inorg. Chem.* 1994, **33**, 5721.
27 W. Carillo-Cabrera, H. Borrmann, S. Paschen, M. Baenitz, F. Steglich, Yu., Grin, *J. Solid State Chem.*, 2005, **178**, 715.
28 H. Menke, H. G. V. Schnering, *Z. Anorg. Allg. Chem.* 1973, **395**, 223.
29 E. Reny, S. Yamanaka, C. Cros, M. Pouchard, *Chem. Commun.*2000, **24,** 2505.
30 N. Jaussaud, M. Pouchard, P. Gravereau, S. Pechev, G. Goglio, C. Cros, A. S. Miguel, P. Toulemonde, *Inorg. Chem.,* 2005, **44**, 2210.
31 K. Kishimoto, K. Akai, N. Muraoka, T. Koyanagi, M. Matsuura, *Appl. Phys. Lett.* 2006, **89**, 172106.
32 W. Carrillo Cabrera, J. Curda, H.G. von Schnering, K. Peters, S. Paschen, M. Baenitz, Yu. Grin, *Z. Kristall*ogr. *NCS*, 2000, **215**, 321-322
33 C. Candolfi, U. Aydemir, A. Ormeci, W. Carrillo-Cabrera, U. Burkhardt, M. Baitinger, N. Oeschler, F. Steglich, andYu. Grin, *J. App. Phys.* 2011, **110**, 043715.
34 A. Czybulka, B. Kuhl, H. U. Schuster, Z. Anorg. Allg. Chem. 1991, **594**, 23.
35 R. L. Firor, K. Seff, *J. Am. Chem. Soc.*, 1977, **99**, 4039.
36 T. B. Reed, D.W. Breck, *J. Am. Chem. Soc.* 1956, **78**, 5972.
37 G. M. Sheldrick, SHELXL-2014 Program for crystal structure refinement, University of Göttingen, Germany, 2014.
38 Shape Software, Atoms V 6.0, Standard Edition, Key Version 1, 2002.
39 L. G. Akselrud, P. Yu. Zavalii, Yu. Grin, V. K. Pecharsky, B. Baumgartner, E. Wölfel, *Mater. Sci. Forum*, 1993, **133-136**, 335.
40 G. Kresse and J. Furthmuller, *Phys. Rev. B,* 1996, **54**, 11169.
41 P. Perdew, K. Burke, M. Ernzerhof, Generalized Gradient Approximation Made Simple, *Phys. Rev. Lett.* 1996, **77**, 3865.
42 M. Beekman, W. Schnelle, H. Borrmann, M. Baitinger, Yu. Grin, G. S. Nolas, *Phys. Rev. Lett.* 2010, **101**, 018301.
43 H. Zhang, J. T. Zhao, M.B. Tang, Z. Y. Man, H. H. Chen, X. X. Yang, *J. Alloys. Comp.* 2009, **476**, 1.
44 H. Zhang, J. T. Zhao, M. B. Tang, Z. Y. Man, H. H. Chen, X. X. Yang, *J. Phys. Chem. Solids,* 2009, **70**, 312.
45 H. Zhang, H. Borrmann, N. Oeschler, C. Candolfi, W. Schnelle, M. Schmidt, U. Burkhardt, M. Baitinger, J. T. Zhao, Yu. Grin, *Inorg. Chem.* 2011, **50**, 1250.
46 H. Zhang, M. Baitinger, L. Fang, W. Schnelle, H. Borrmann, U. Burkhardt, A. Ormeci, J. T. Zhao, Yu. Grin, *Inorg. Chem.* 2013, **52**, 9720.
47 C. Gatti, L. Bertini, N. P. Blake, B. B. Iversen, *Chem. Eur. J.* **9** , 4556-4568 (2003).